Strojniški vestnik – Journal of Mechanical Engineering, Volume 66, Issue 1, January 2020, pp. 15-28
DOI:10.5545/sv-jme.2019.6002

Heat dissipation from stationary passenger car brake discs

Stergios Topouris[1], Dragan Stamenković[2], Michel Olphe-Galliard[1], Vladimir Popović[2], Marko Tirović[1]*

[1]Cranfield University, School of Aerospace, Transport and Manufacturing, Cranfield, UK
[2]University of Belgrade, Faculty of Mechanical Engineering, Belgrade, Serbia

* Corresponding Author, dstamenkovic@mas.bg.ac.rs

Abstract

Experimental investigation of the heat dissipation from stationary brake discs concentrated on four disc designs, a ventilated disc with radial vanes, two types of ventilated discs with curved vanes - a non-drilled and cross-drilled disc, and a solid disc. The experiments were conducted on a purpose built Thermal Spin Rig and provided repeatable and accurate temperature measurement and reliable prediction of the total, convective and radiative heat dissipation coefficients. The values obtained compare favourably with Computational Fluid Dynamics results for the ventilated disc with radial vanes and solid disc, though the differences were somewhat pronounced for the ventilated discs. The speeds of the hot air rising above the disc are under 1 m/s, hence too low to experimentally validate. However, the use of a smoke generator and suitable probe was very useful in qualitatively validating the flow patterns for all four disc designs.

Convective heat transfer coefficients increase with temperature but the values are very low, typically between 3 and 5 W/m^{2}K for the disc designs and temperature range analysed. As expected, from the four designs studied, the disc with radial vanes has highest convective heat dissipation coefficient and the solid disc the lowest, being about 30% inferior. Convective heat dissipation coefficient for the discs with curved vanes was about 20% lower than for the disc with radial vanes, with the cross drilled design showing marginal improvement at higher temperatures.

Keywords: Brake Disc, Heat Dissipation, Convective Cooling, Computational Fluid Dynamics, Natural Convection

NOMENCLATURE

Symbol	Description	Unit
A_w	Total disc wetted area	[m^2]
A_{rad}	Radiative heat dissipation disc area	[m^2]
c_p	Specific heat of disc material (grey iron)	[J/kgK]
h_{tot}	Total average heat transfer coefficient	[W/m^2K]
h_{conv}	Average convective heat transfer coefficient	[W/m^2K]
h_{rad}	Average radiative heat transfer coefficient	[W/m^2K]
m	Disc mass	[kg]
T_d	Average disc temperature during time period $(t_1 - t_2)$	[K]
T_{d1}	Disc temperature at the time t_1	[K]
T_{d2}	Disc temperature at the time t_2	[K]
T_∞	Ambient air temperature	[K]
t	*Time*	[s]
ε	Disc surface emissivity	[-]
σ	Stefan-Boltzmann constant (5.67×10^{-8})	[W/m^2K^2]

1. Background

Brake cooling is vital for safe vehicle operation and has attracted substantial research from very early days, however most research and published data relate to heat dissipation from rotating discs. Cooling of a stationary brake is equally important as many critical cases are related to this driving condition. For instance, brake fluid is much more likely to boil if the vehicle is not moving. The consequences can only become apparent once the vehicle starts moving again, making the situation safety critical. Convective heat dissipation is drastically reduced, from predominantly forced cooling (at high air speeds) to natural convection only (air speed being zero). Instead of the heat being dissipated to the surrounding air, which is propelled away from the brake, much more heat is being transmitted to pads and caliper through conduction and radiation. Furthermore, considerable portion of the heat being dissipated form the disc by natural convection is heating the caliper as the hot air is forced upwards by the natural convection. The air surrounding the brake assembly is 'trapped' within the wheel and wheel arch cavities and the brake ambient temperature is rapidly increasing, well above the outside ambient air temperature.

The situation might be equally critical during 'hot parking', when the vehicle is parked after heavy brake use. In such conditions some brake components can reach higher temperatures than for a moving vehicle. Traditionally, the risks with 'hot parking' were related to boiling of brake fluid, however vehicle 'roll away' is another potentially critical condition. As the disc and pads cool down they 'shrink' (their thickness reduces) whereas the caliper expands as it heats up as a result of a heat transferred from the pads and disc. This leads to the reduction of the clamp force, causing decrease in friction force (braking torque) and potentially leading to rollaway if the vehicle is parked on a gradient. The condition is most critical when installing Electric Parking Brake (EPB) where long flexible cables are not used and there is no flexibility in the system to compensate for reduction in disc and pad thickness. EPB has brought hot parking to an entirely new level, ensuring safe vehicle parking on a gradient (being specified at 20% by ECE Regulation 13H). The methodologies used to cope with this challenge include 'over-clamping' (i.e. applying much higher force than required in order to 'stretch' the caliper which should compensate for disc and pad shrinkage) and re-parking (i.e. re-applying the brake automatically after the vehicle has been parked).

With the installation of electric and electronic components into calipers (EPB, 'low drag' calipers etc.), there is a potential danger with overheating and permanent damage to these parts, hence accurate prediction of brake temperature in parking conditions is becoming even more important.

Heat dissipation from stationary brake is also important for accurately predicting brake temperatures in drive cycles which contain periods when the vehicle is stationary. Though these cycles are typically not safety critical from the brake performance point of view, brake temperatures are important in understanding and minimising residual drag, providing good brake pedal feel and reliably estimating brake wear.

Finally, braking of Hybrid and electric vehicles (HEVs) imposes another braking challenge, in addition to complexities related to brake pedal feel, residual drag and EPB. The ECE Regulations 13H require all braking tests (such as repeated brake applications – 'fade and recovery') to be successfully performed by friction brakes only, without the use of regenerative braking. Considering HEVs are typically heavier than equivalent cars with internal combustion engines only, understanding braking requirements is paramount not only regarding safety but also in order to minimize brake mass and resolve brake cooling in the most effective way for both moving and stationary vehicle operation. Though some of

these vehicles are relatively low performance, there are some extremely high performance HEVs with very rapid acceleration characteristics and therefore very high braking demands.

When analysing brake thermal aspects in parking conditions, it should be pointed out that critical cooling times can be quite prolonged, for passenger cars with 'classical' hand brake designs, the rollaway are known to have occurred up to 30 minutes after the vehicle was parked with hot brakes. This was for 'medium gradients' (~10%) as for the higher gradients the rollaway occurs much quicker. In commercial vehicles, the critical period can be up to 1 hour (Stevens, 2013).

As a first step in studying heat dissipation from stationary passenger car disc brake assemblies, the focus will be on the brake disc. Four types of brake discs will be studied, for two passenger vehicles. The first vehicle is Volkswagen Passat and the second Lotus Elise S2, with the basic vehicle and disc characteristics given in Table 1.

Table 1 Vehicle characteristics

Characteristics	Vehicle	
	VW Passat 2.0T FSI 2007	Lotus Elise S2 2013
Gross vehicle mass [kg]	2100	1141
Static front axle load [kg]	1080	570.5
Static rear axle load [kg]	1020	570.5
Wheelbase [mm]	2709	2300
Maximum engine power [kW]	147	89*
Maximum vehicle speed [km/h]	235	205
Front disc type	Ventilated with radial vanes	Ventilated with curved vanes**
Front disc outer diameter [mm]	321	288***
Rear disc type	Solid	Ventilated with curved vanes**
Rear disc outer diameter [mm]	286	288***

**Basic model*

***Option: Cross drilled*

**** Front and rear discs are identical*

Brake discs are shown in Figure 1, with (a) and (b) presenting VW Passat front and rear discs respectively. Lotus Elise S2 standard disc is marked (c) in Figure 1, with (d) presenting a cross drilled disc. It should be noted that Elise front and rear discs are identical. From Figure 1 it can be noted that all three ventilated discs are of a 'swan neck' type, meaning that the outboard disc friction face is attached to the top hat section but using a 'swan neck' type feature in order to minimise disc coning. This design allows air intake from the inboard side, resulting in good cooling characteristics.

Detailed design characteristics for all four discs studied are presented in Table 2. Front VW Passat disc (a) is the largest and heaviest, owing the high vehicle mass and maximum speed, as well as brake force distribution (Front : Rear) of 2.1 for fully laden vehicle. Solid disc (b) has smallest outer (OD) and inner (ID) diameters, it is thinnest, has smallest wetted area and is also lightest at only 3.2 kg. It is worth pointing out that both vehicles have practically 50:50 static load distribution for fully laden condition. Whereas this substantially changes for unladen state of VW Passat (with much more loaded taken by the front axle in unladen and partly laden conditions), there is practically no difference for Lotus Elise as the engine is mounted in the middle and in addition to the driver, there is only place for one passenger (next to the driver) and very little luggage. Consequently, neither the load nor the distribution per axle change much for Lotus. Without entering into further analyses into brake sizing and characteristics, a

brief literature review will be presented, which will be followed by the modelling and experimental results obtained.

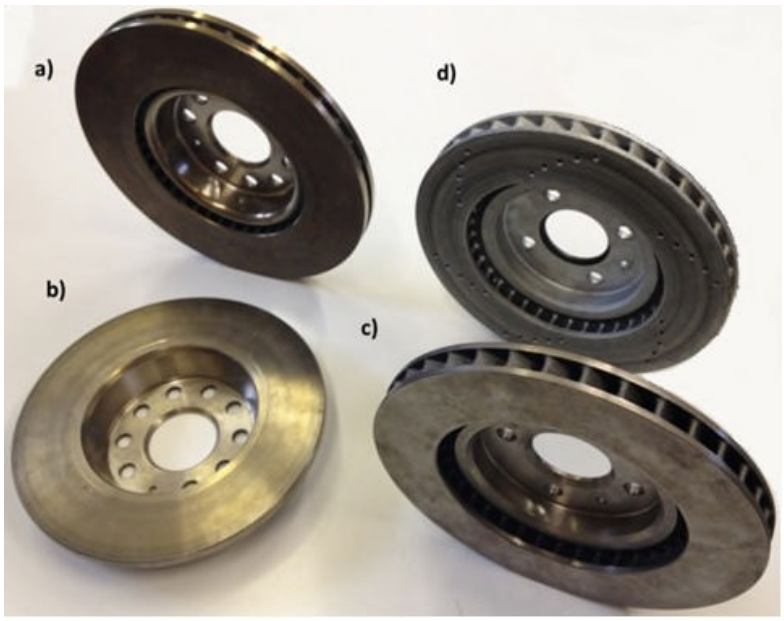

Figure 1 Discs Analysed: VW Passat **(a)** front, **(b)** rear; Lotus Elise S2: **(c)** standard, **(d)** cross drilled

Table 2 Disc characteristics

Ref. Fig. 1	**Type / Design**	**OD** x **ID** x **Thickness** [mm]	**Number of vanes** [-]	**Wetted area** [m^2]	**Mass** [kg]
a)	Ventilated with radial vanes	321 x 188 x 25	40	0.3086	9.40
b)	Solid	286 x 180 x 12	N/A	0.1678	3.20
c)	Ventilated with curved vanes	288 x 185 x 26	37	0.2562	4.20
d)	Ventilated with curved vanes, cross drilled	288 x 185 x 26	37	0.2586	4.18

2. Literature review

Due to its importance for safe vehicle operation, heat dissipation attracted considerable research from the early days. However, complex geometry, installation, boundary conditions and service duties limited the application of analytical methods and the work was predominantly experimental, aiming at measuring maximum brake temperatures at specific duties. The research was also mostly concerned with rotating discs, with analytical methods applied initially to a geometrically perfect disc shape (not an actual brake disc) rotating in still air (Wagner, 1948), and in a cross flow (Cobb and Saunders, 1956; Richardson and Saunders, 1963). Newcomb (1959) and Newcomb and Spurr (1967), investigated experimentally heat dissipation from brake discs installed on vehicles, with the aim of establishing relationships and finding effective solutions in predicting brake disc temperatures. The ability in modelling the actual brake geometry came with the development of numerical methods (Finite Element and Finite Difference) but the complexity of boundary conditions still required substantial experimental work in establishing and validating temperature prediction procedures. Substantial contributions have

been provided by Noyes and Vickers (1969), Morgan and Dennis (1972), Limpert (1975) and Sisson (1978).

Only with the development of Computational Fluid Dynamics (CFD) the actual boundary conditions, i.e. convective heat transfer coefficients can be reliably theoretically predicted. Still, it took some time for these methods to be sufficiently developed for successful analyses of brake discs. Complex geometry, boundary conditions and disc rotation required robust algorithms and very powerful computers to deal with models having millions of cells. Stationary disc analysis was not any easier to model. The disc does not rotate but the energy for air flow is provided by change in air density due to its heating and expansion. Some useful CFD work for rotating disc analysis and optimisation for automotive and railway discs is provided by Daudi (1999), Galindo-Lopez and Tirovic (2008, 2013), Pevec et al. (2012), Son et al. (2018) and others.

The only research known to the authors dealing with CFD modelling in predicting temperatures and heat transfer coefficients for a stationary disc, is published by Stevens (2013), Stevens and Tirovic (2018) and Tirovic and Stevens (2018). The conclusions are multi fold but can be summarised in that effective CFD modelling of the stationary discs is possible nonetheless it requires large meshes and extreme care in their creation (in particular when modelling boundary layers). Obviously, powerful computers are needed and CPU times are considerable (typically over 48 hours). The most suitable turbulence model was found to be SST in terms of both accuracy and speed. The values of convective heat transfer coefficients are similar but higher than the values quoted in this paper. This is due to much larger discs (outer dimeter being 434 mm) heated to higher temperatures (over 350°C). It was also concluded that flow patterns change with temperatures and static disc cooling at higher temperatures can be reduced by the hot air exiting lower ventilation channels and blocking air entry into upper channels. This phenomenon was typical for large anti-coning type discs studied but some evidence of similar effects has been also detected by the authors and will be presented and discussed later. The analyses (Stevens, 2013) also employed analytical methods for heat transfer from surfaces (walls and cylinders), developed by McAdams (1954), Morgan (1975), Churchill and Chu (1975) and Necati Özisik (1989). Very useful results have been obtained for a wide temperature range, but these are limited to solid discs only.

Convective heat dissipation prediction in friction brakes has been vastly improved in recent years nonetheless still considerably relies on experimental work. This is not limited to this mode of heat dissipation only but also to radiative and conductive losses. Both these modes are speed independent and the radiation is highly temperature dependent. Consequently, appropriate modelling of these two modes is vital for accurate prediction of convective losses and brake temperatures in any operating duty. Substantial work and contribution in effectively tackling these modes has been published by Tirovic and Voller (2005) and Teimourimanesh et al. (2014) for conductive heat transfer and by Eisengräber et al. (1999) and Dufrenoy et al. (2018) for radiation. Accurate and reliable heat dissipation is required not only for safe prediction of brake temperatures regarding friction characteristics (fade) and brake components and fluid temperatures, it has much wider implications in lightweight designs and NVH characteristics, as presented by Grieve et al. (1998) and Tang et al. (2018) respectively.

3. Experimental set-up

All tests presented in this paper were conducted on a specially designed Spin Thermal Rig, with its CAD model show in Figure 2. The Rig has an in-line arrangement of the motor, coupling, drive shaft and brake disc, with suitable bearing housing placed on a supporting frame/table. Figure 3 shows the actual Rig.

The operational procedure has three distinctive phases:

a) Heating period

The disc is rotating at low speed (~ 100 rpm) and the heater box is placed over the disc (see Figure 3b) and hot air guns activated, providing a gradual, uniform disc heating. Once the disc reaches the required temperature, typically around 250 °C, the heating is turned off, with the disc continuing to rotate at low speed. Temperatures and other variables are logged during this period but typically not processed.

b) Soaking period

The disc is continuing to rotate at low speed for several minutes in order to equalise the temperatures. All variables are logged during this period for monitoring purpose but not typically processed. At the end of this period the heating box is removed.

c) Cooling down period

This period starts after the soaking period and all variables are logged and processed during this period. The disc is typically cooled down to under 50°C. Disc surface temperatures logged during this period are the actual 'cooling curves' and used to calculate average heat transfer coefficients.

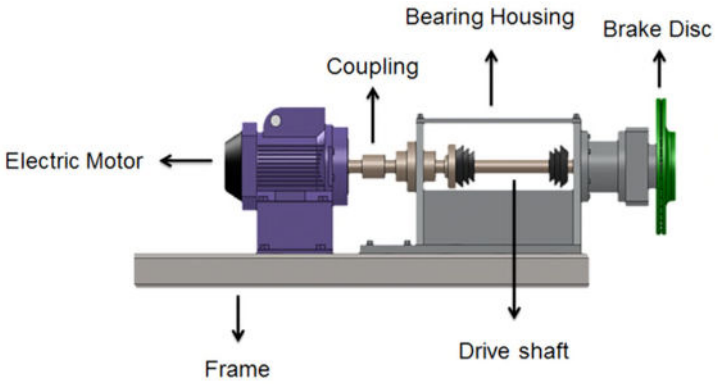

Figure 2 Disc Thermal Spin Rig concept

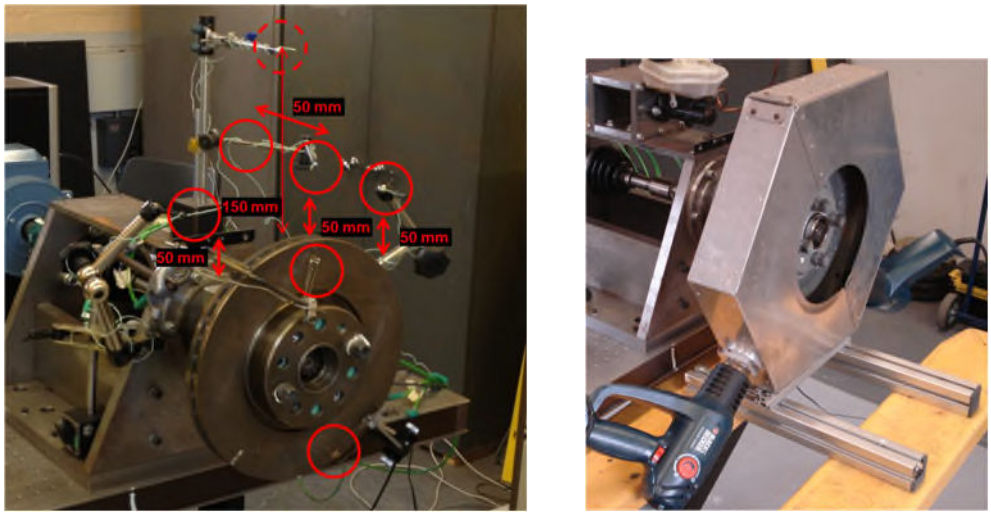

a) **b)**

Figure 3 Thermal Spin Rig: **(a)** thermocouples installed and **(b)** heating box

The instrumentation used (see Figure 3a) consisted of a number of rubbing/contact thermocouples (Figure 4a, K Type, supplied by TC Direct) which were positioned around the disc, contacting disc friction surfaces. It should be pointed out that differences in measured disc temperatures across friction surfaces were very small. This is a result of low cooling rate and thick disc faces made of thermally highly conductive grey cast iron. Figure 3a, shows two contact thermocouples positioned 30 mm radially from the disc outer diameter, on the bottom and top of the outboard friction face. Two more thermocouples were placed at the same nominal position on the inboard friction surface. Temperature of the air in the plume above the disc was measured using 5 thermocouples, positioned above the disc, as shown in Figure 3a, using wire type thermocouples (Figure 4b, also K Type). Ambient temperature was measured in 4 places around the laboratory and all doors and windows were closed to prevent any air movement.

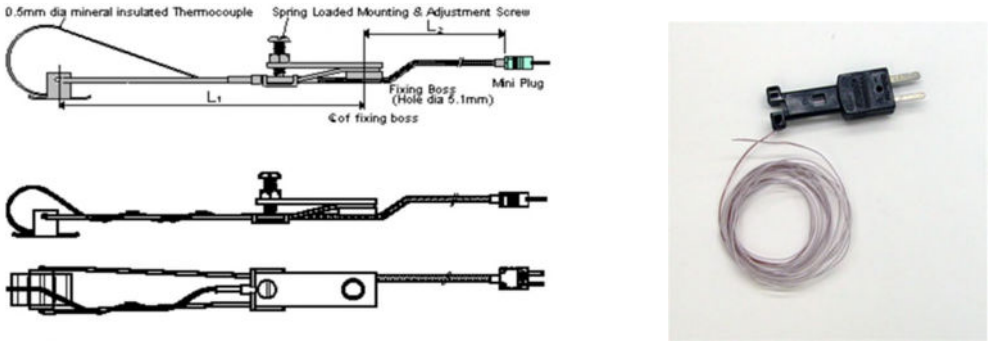

a) **b)**

Figure 4 Thermocouples used: **(a)** Rubbing/Contact thermocouple and **(b)** Wire thermocouple

a) **b)**

Figure 5 National Instruments equipment: **(a)** CompactDAQ and **(b)** Thermocouple Module

For signal conditioning and data logging, National Instruments CompactDAQ was used (Figure 5a) connected to a PC, together with Thermocouple modules NI 9211 (Figure 5b). The developed code enabled direct temperature measurement and display during the cooling period, as well as presentation of the entire cooling event, as shown in Figure 6. It can be noticed that all temperatures are very close and the cooling curves are smooth. Consequently, the temperatures can be suitably averaged and reliably used to calculate average heat transfer coefficients. The tests were repeated numerous times and practically identical values were obtained. More details about the methodology, uncertainty and the results are available by Topouris (2017) and Stevens (2013).

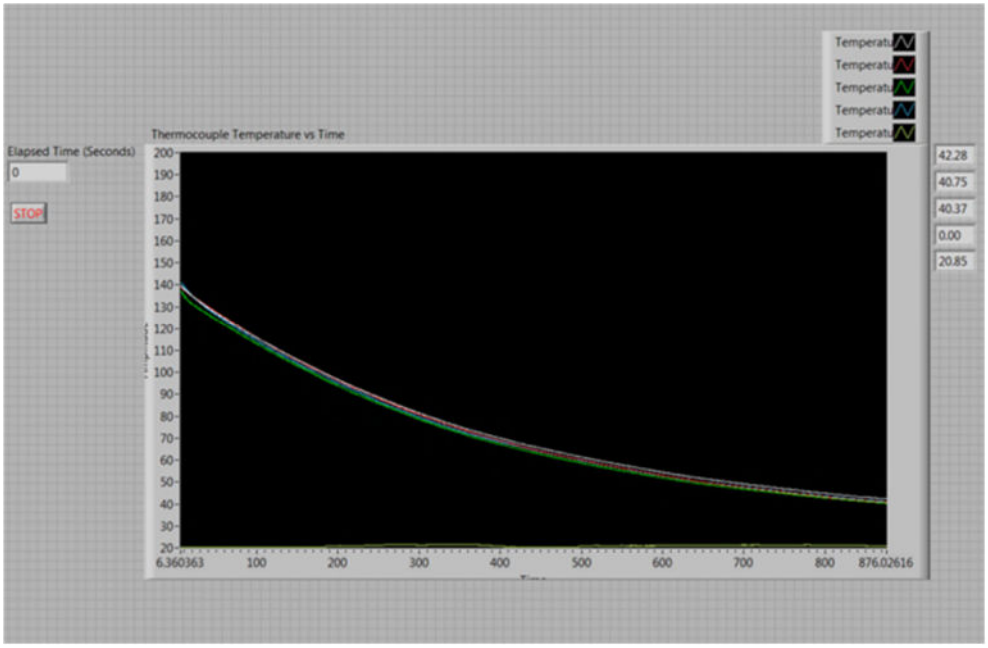

Figure 6 Cooling curves example using contact (rubbing) thermocouples

In order to try and obtain more temperature data across the friction face and hub flange area of the disc, thermal imaging camera FLIR A320 was also used (Figure 7a), with Figure 7b showing the image and selected points for obtaining 'spot' temperatures. Unfortunately, this was not providing useful results, as minor differences in disc surface condition lead to small differences in emissivity values, which in turn caused differences in obtained temperature readings. The differences were typically around 5°C but sometimes higher even 10°C or more, without any reason for the difference (except change in emissivity) and with contact thermocouples showing identical temperatures in these areas. Still the cooling curves were smooth and averaging was possible. However, such differences in local temperatures were typically reducing but not diminishing as disc was cooling down and even existed when the disc was approaching or reaching ambient temperature. Though the use of infrared camera for temperature measurements of fast rotating discs at high temperature was found useful by some authors and recently much improved by Dufrenoy et al. (2018), for the considered disc, the temperature range and stationary cooling condition this method was not considered suitable.

In order to compare the results with Computational Fluid Dynamics (CFD) predictions, an attempt was made to measure air temperatures of the plume above the disc, using wire thermocouples shown in Figure 4b, with the positions marked in Figure 3a. Unfortunately, this approach was found to be unsuitable. The temperature variations were irregular ('erratic'), despite every effort in preventing air movement in the laboratory. It is interesting to point out that Stevens (2013) found this method reliable but for much larger and heavier discs, heated to higher temperatures.

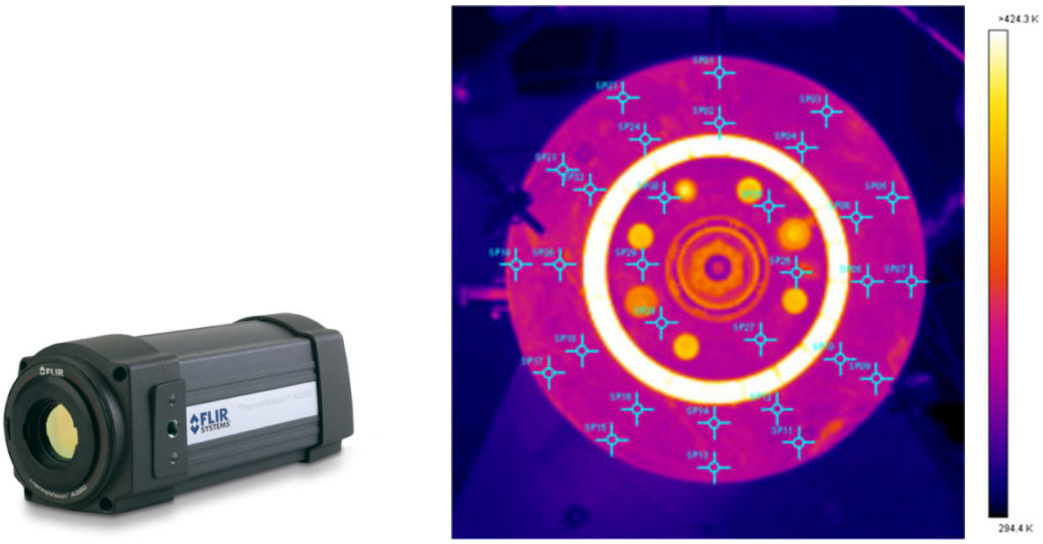

Figure 7 Infrared temperature measurements:
(a) FLIR A320 Camera and **(b)** full field disc thermal image and selected points
(b)

The problems with better understanding stationary disc cooling is not related to temperature measurements only. As it will be shown, air speeds within the plume rising above the disc are also very low, typically under 1 m/s, making the air speed measurements practically impossible. Consequently, disc surface temperatures measured using contact thermocouples was found to be the only reliable method and these results were used to calculate average heat transfer coefficients, which will be compared with CFD results As it will be shown later, some very useful but qualitative (only) indications of the flows were obtained using smoke generator.

4. Calculation of average heat transfer coefficients from measured temperatures

As explained in the previous section, during the cooling period there is no heat input. Therefore, the energy dissipated during the time period t_1 to t_2 will be equal to the thermal energy loss from the disc. Consequently the average total heat transfer coefficient $\boldsymbol{h_{tot}}$ can be defined as:

$$\boldsymbol{h_{tot} = -ln\left(\frac{T_{d2} - T_\infty}{T_{d1} - T_\infty}\right)\frac{mc_p}{A_w(t_2 - t_1)}} \tag{1}$$

where:

T_{d2}	is disc temperature at the time t_2;
T_{d1}	is disc temperature at the time t_1;
T_∞	is ambient temperature;
m	is disc mass;
c_p	is specific heat of disc material (grey iron)
A_w	is total disc wetted area.

The average coefficient of heat transfer due to radiation during the period $(t_2 - t_1)$ can be defined as:

$$\boldsymbol{h_{rad} = \varepsilon\sigma\left(\frac{A_{rad}}{A_w}\right)\left(\frac{T_d^4 - T_\infty^4}{T_d - T_\infty}\right)}$$

(2)

where:

- ε is disc surface emissivity;
- σ is Stefan-Boltzmann constant;
- A_{rad} is radiative heat dissipation disc area;
- T_d is average disc temperature during the period $(t_2 - t_1)$.

Accordingly, the average convective heat transfer coefficient, for the period $(t_2 - t_1)$, can be calculated as:

$$\boldsymbol{h_{conv} = h_{tot} - h_{rad}} \quad (3)$$

As the disc cools down, temperature will drop slower, hence keeping the same time periods $(t_2 - t_1)$, for calculating average heat dissipation coefficients may not be the best approach. It was found very useful to keep the temperature differences $(T_2 - T_1)$ constant for conducting these calculations. Typically temperature differences of around 20°C are considered most suitable, providing reliable disc surface temperatures and sufficiently short periods to account for highly non-linear influence of radiative heat losses. In order to determine disc surface emissivity, thermal camera (explained above) was used and the temperature measured at the same time in the close proximity to the predefined points using contact thermocouples. After extensive surface mapping an average emissivity value was established for the entire disc surface. There were some variations between discs (which were taken into consideration when processing the data) but the overall average value was found to be $\varepsilon = 0.82$. It should be pointed out that disc surface was oxidised, covered in fine corrosion after repeated heating and cooling. There were no pads to polish the disc surface and contact/rubbing thermocouples covered only small area and caused little change to the surface emissivity in the contact paths with the disc (as the disc was rotating during heating period but the speeds and interface pressures were very low).

5. CFD Modelling and comparison with experimental results

CFD modelling for VW front and rear disc was conducted using CFX code (for more details see Olphe-Galliard, 2011).

5.1. CFD Mesh

Figure 8 depicts front ventilated disc model, with |Figure 8a showing the air domain, 8b and 8c surface mesh on the outboard and inboard side respectively. Mesh detail in the area of channel entrance at disc inner diameter is shown in Figure 8d, where very fine mesh, with numerous small cells can be observed.

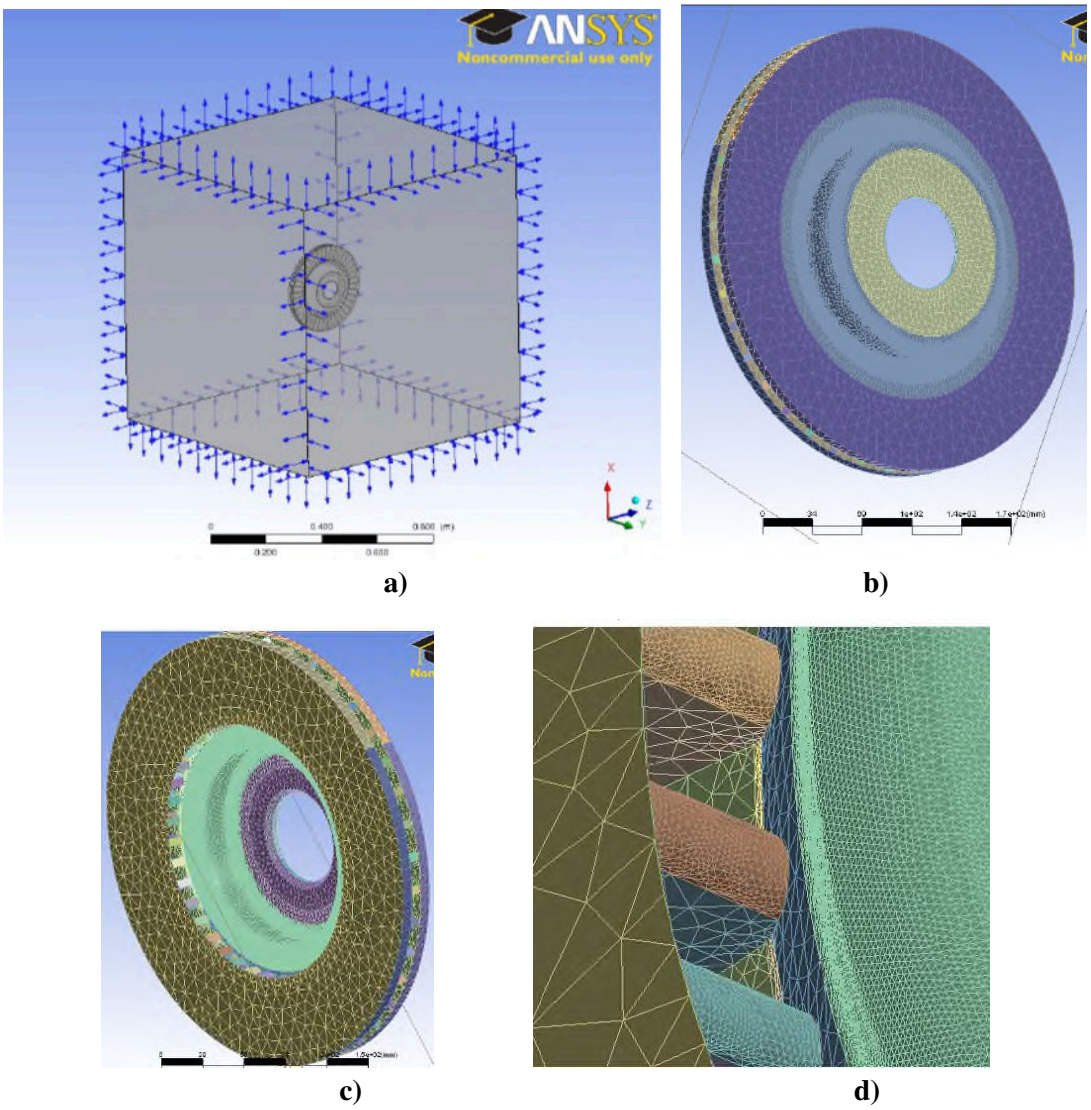

Figure 8 CFD Modelling of the ventilated disc: **(a)** air domain; **(b)** and **(c)** surface mesh; **(d)** mesh detail

Figure 9 shows rear solid disc, where the mesh did not require that many cells. Mesh statistics, for the two discs, is included in Table 2. The total number of cells was over 12 million for the ventilated and over 3 million for the solid disc. It should be pointed out that such a fine mesh was necessary for modelling air flow and heat transfer of stationary discs. Much lower number of cells were needed when modelling rotating disc or disc in a cross flow. *K-ε* turbulence model was used for both discs and the results will be firstly presented alongside qualitative experimental investigations using smoke generator.

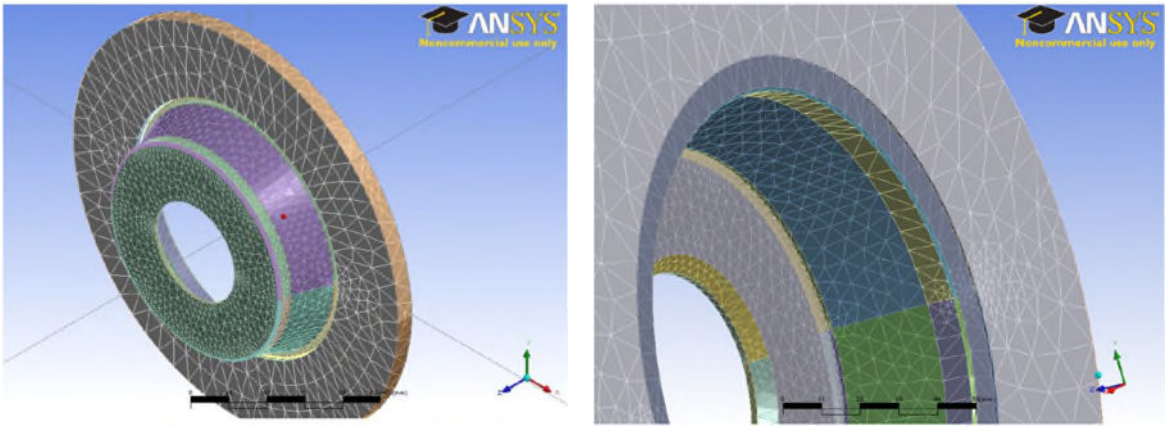

a) **b)**

Figure 9 CFD Modelling of the solid disc: **(a)** surface mesh; **(b)** mesh detail

Table 2: CFD Mesh statistics; (Olphe-Galliard, 2011) (Olphe-Galliard, 2011)

Characteristic	Ventilated disc (fine mesh)	Solid disc
Total number of nodes	3 295 654	857 655
Total number of elements Of which:	12 117 247	3 226 623
Tetrahedral	8 825 745	2 406 319
Pyramids	112	287
Prisms	3 291 390	820 017

5.2. Air flow

Figure 10a shows air velocity contours for the ventilated disc at 250 °C in the middle vertical (XZ) plane. It can be seen that the maximum velocity predicted is just over 0.9 m/s, therefore it was not possible to conduct experimental validation. In order to validate flow pattern, tests were conducted using smoke generator with neutral buoyancy smoke (generated from special oil), with the fine probe releasing the smoke in various areas in the proximity to the disc. Figure 10b shows the plume rising from the disc faces and channels, which closely resembles the CFD predictions displayed in Figure 10a. It should be pointed out that unfortunately the disc could not be heated to 250°, the temperature used for CFD modelling. The flow air patterns (such as Figure 10b) are very difficult to photograph and obtain clear flow indications. The best approach established was to take videos and then play them frame by frame and select the clearest pictures with the highest contrast. This approach inevitably reduced picture resolution, with the disc cooling down during filming. The light also played an important part in taking useful images - too much or too little light made the smoke practically invisible or air plume direction difficult to understand. As expected, the cooling is most effective in the upper side of the disc, and least effective in the channels which are in the horizontal position.

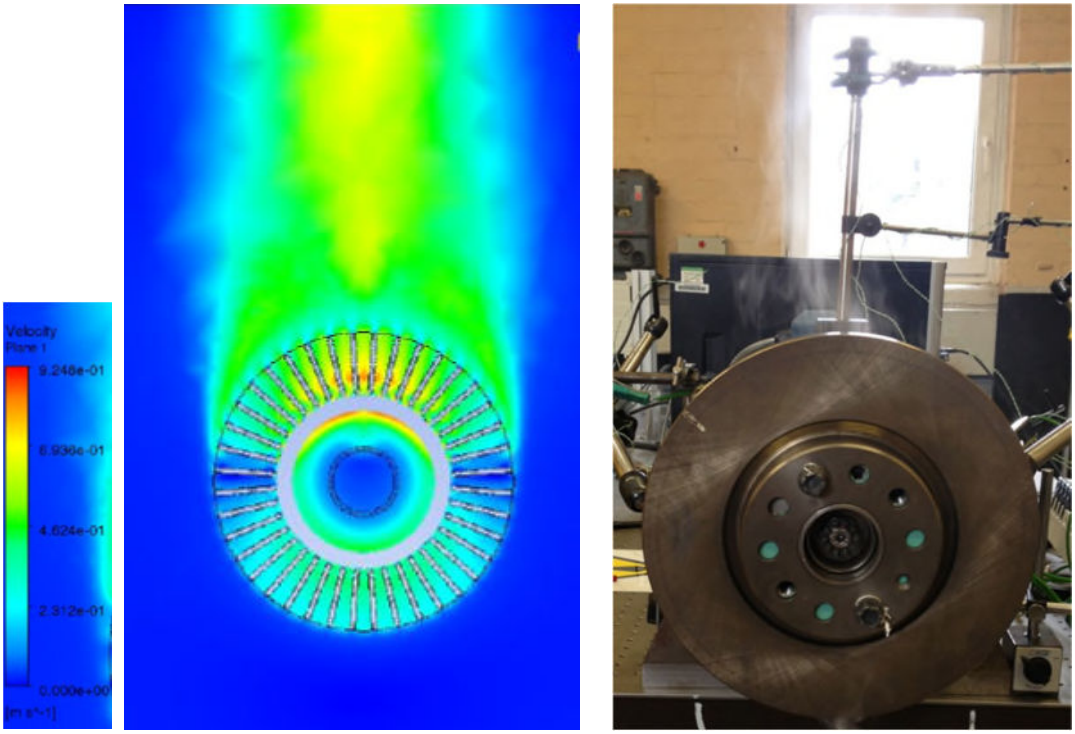

a) **b)**

Figure 10 Ventilated disc: (a) CFD air velocities and (b) flow (smoke) pattern using smoke generator

Figure 11a shows air velocity contours in the vertical plane YZ running through the disc axis, with 11b showing horizontal plane XY, again running through the disc axis. It can be noticed that upwards air flow in the swan neck area, at disc ID, blocks air entry into the ventilation channels. This phenomenon (effect) diminishes with drop in disc temperatures. As a result, convective cooling does not drop as drastically as probably expected with disc cooling, owing to (proportionally) more air flow going through ventilation channels at lower disc temperatures.

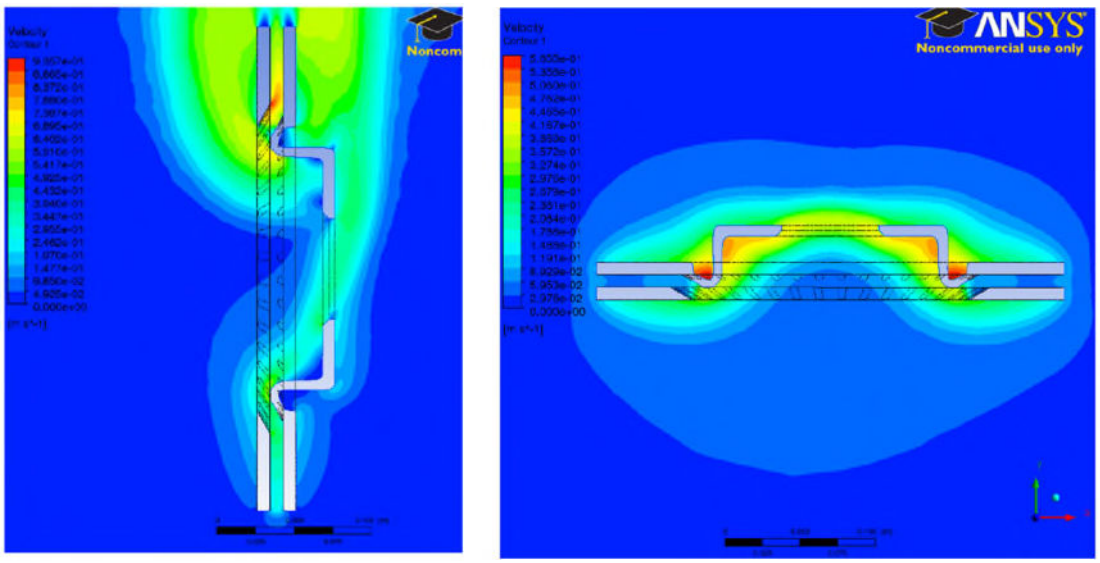

a) **b)**

Figure 11 Ventilated disc predicted air velocity contours at 250°C: **(a)** YZ plane and **(b)** XY plane

Figure 12 shows the solid disc. Again, CFD analyses were performed for 250°C and experiments at 150°C due to the limitation of the heating system. CFD air velocities are shown in the line form (Figure 12a) and all indications are that the flow pattern matches very well with the visualisation using smoke generator shown in Figure 12b. The maximum air speeds predicted were just over 0.6 m/s, more than one disc diameter above the disc, in the middle plane. Unfortunately, this value is very low and could not be experimentally verified but the smoke rising above the disc (Figure 12b) clearly indicates the same pattern and position of the highest speed.

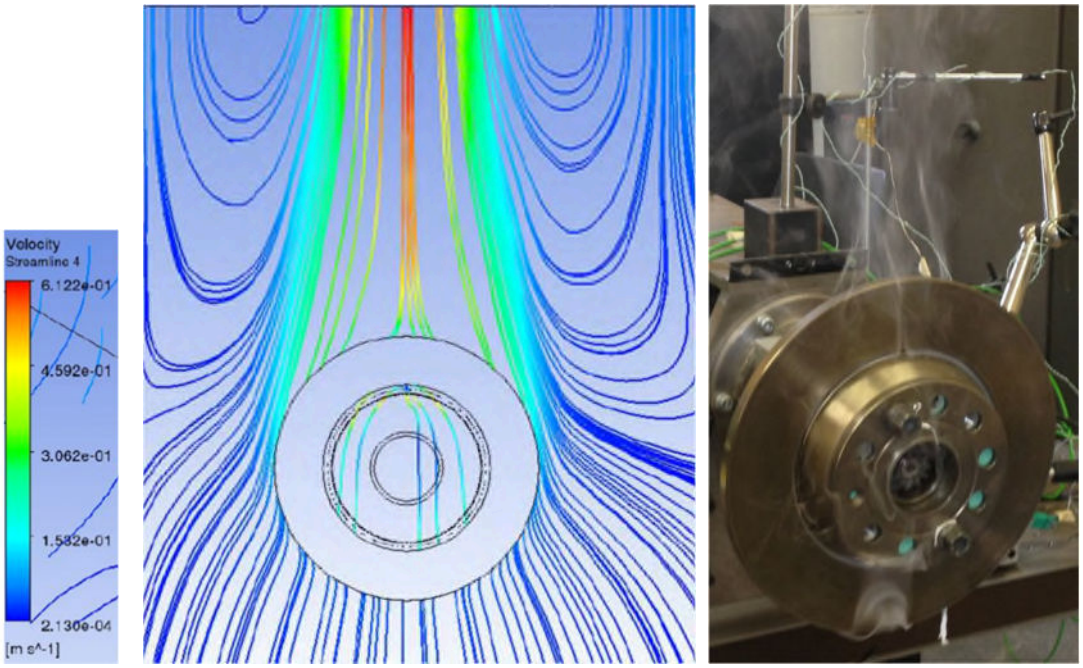

a) **b)**

Figure 12 Solid disc: **(a)** CFD air velocities; and **(b)** Flow (smoke) pattern using smoke generator

5.2 Air temperatures

Despite not being able to accurately measure air temperatures, it is useful to look at the CFD results shown in Figure 13 for the ventilated (13a) and solid (13b) discs at 250°C (note the air temperature is shown in degrees Kelvin). Air temperature seems to rapidly drop after rising above the disc. The plume is also relatively narrow. That probably best explains why the efforts in measuring air temperature was not successful in this case, whereas Stevens (2013) successfully measured air temperatures but for much larger and heavier commercial vehicle brake discs heated to higher temperatures. The air temperatures shown in Figure 13 match well with the air speed and flow patterns shown in Figures 10, 11 and 12.

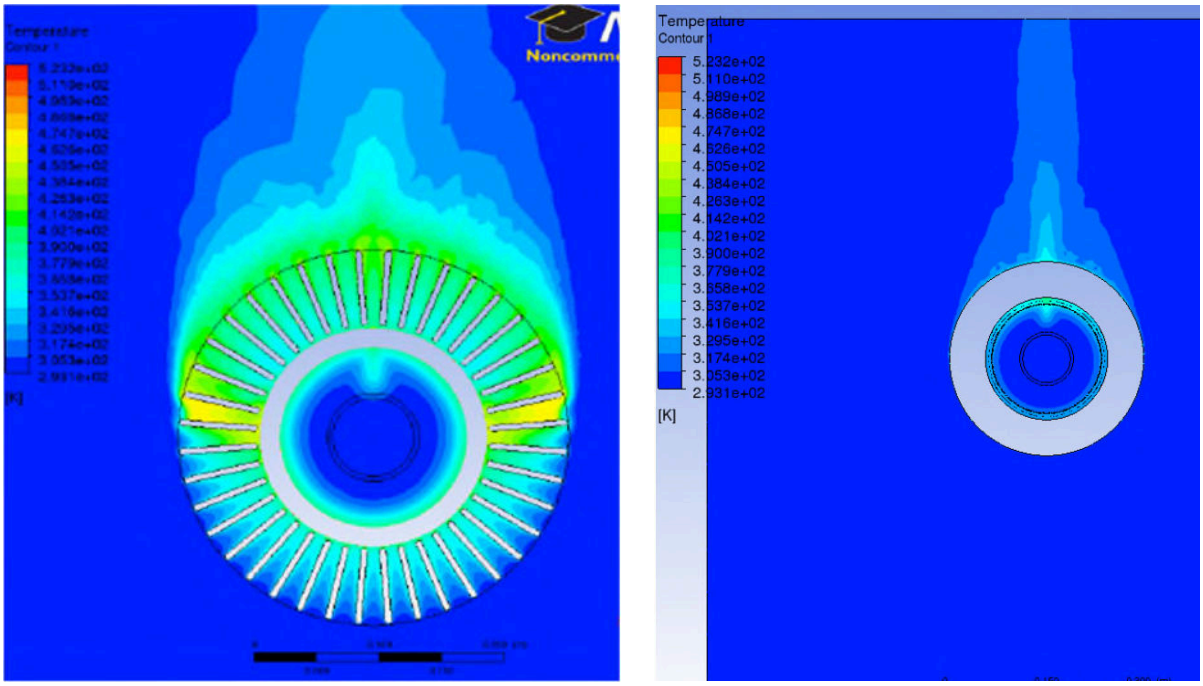

a) **b)**

Figure 13 Air temperature contour in XZ plane for discs at 250°C: **(a)** Ventilated and **(b)** Solid disc;

5.3 Heat transfer coefficients

CFD analyses also enabled predictions of the local and average convective heat transfer coefficients over the disc surfaces, with Figure 14 showing the ventilated and Figure 15 solid disc. For both designs it is clear that convective heat dissipation is more effective from the upper part of the disc, as it would be expected. On the outboard side of the disc the effect of the hub (top hat) can also be observed. The flow is blocked and there is a reduction of the convective cooling in the middle of the disc, above the hub. However, this effect is not present on the inboard side of the disc friction faces. Maximum values of the heat transfer coefficient reach approx. 14.8 W/m^{2}K for the ventilated disc (Figure 14) and 8.2 W/m^{2}K for the solid disc (Figure 15) but these values of the convective heat transfer coefficients are limited to very small areas with no practical significance to disc cooling. For both designs, the highest values covering larger disc areas are around 5 W/m^{2}K. CFD analyses enabled automatic calculations of average values for the convective heat dissipation coefficients, from the distributions shown in Figures 14 and 15.

Experimental investigations enabled only the extractions of average convective heat dissipation coefficients, from the average cooling curves (measured surface temperatures during disc cooling). The measurements of disc surface temperatures proved to be very repeatable and reliable. The procedure for calculating average convective heat transfer coefficients from cooling curves was explained earlier on, which now enables for these values to be compared with CFD results. To cover the temperature range, CFD analyses had to be repeated for lower temperatures. The comparisons presented in Figures 16 and 17 for ventilated and solid discs respectively, show quite interesting phenomena. For the ventilated disc (Figure 16), the average convective heat transfer coefficients calculated from the measured cooling curves have higher values than CFD predictions. The gradient is also steeper, the cooling is becoming more effective with increase in disc temperature. Unfortunately, with the heating system available it was not possible to heat the disc to higher experimental temperatures but for disc at around 100°C, the

experimental values are about 40% higher. For the solid disc (Figure 17) experimental and CFD values of the convective heat transfer coefficient are much closer. Experimental values are again higher but only by about 8%. Though the experiments and CFD analyses were conducted for the same discs and nominal conditions, there were differences in 'holding' the discs, as the discs were completely free standing in still air in CFD analyses (see Figures 8a and 9a), whereas they were mounted to the hub flange and in proximity to the upright in experiments (see Figure 3a).

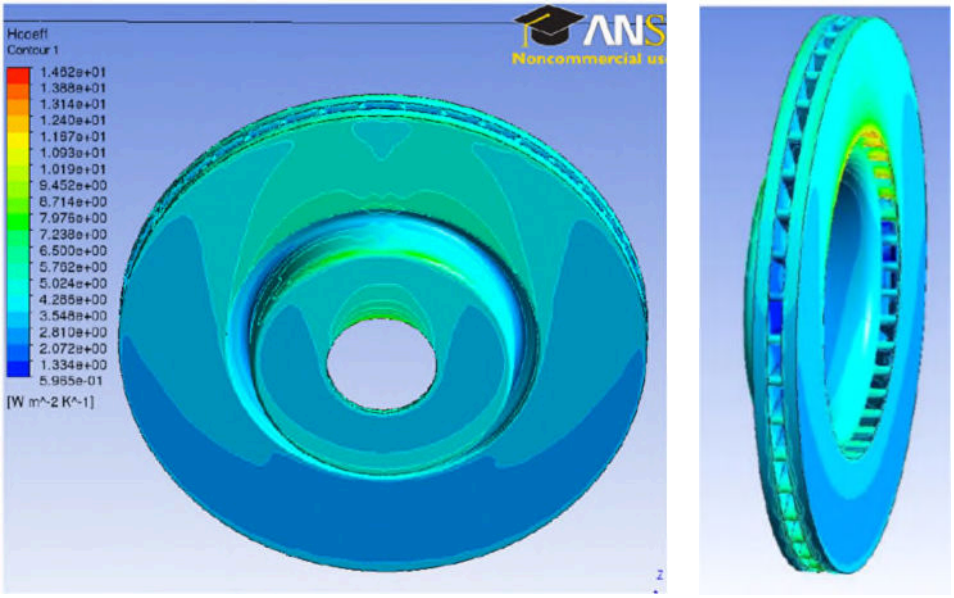

Figure 14 Predicted convective heat transfer coefficient distribution for ventilated disc

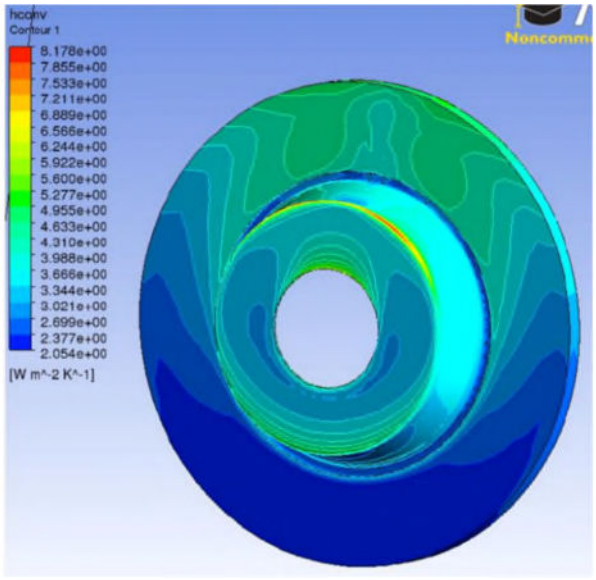

Figure 15 Predicted convective heat transfer coefficient distribution for solid disc

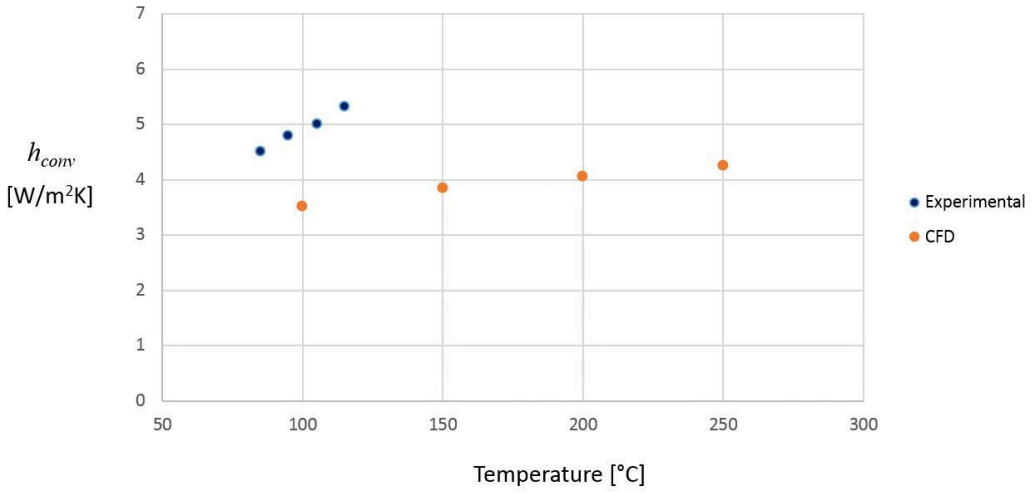

Figure 16 Ventilated disc: Experimental and CFD average convective heat transfer coefficients

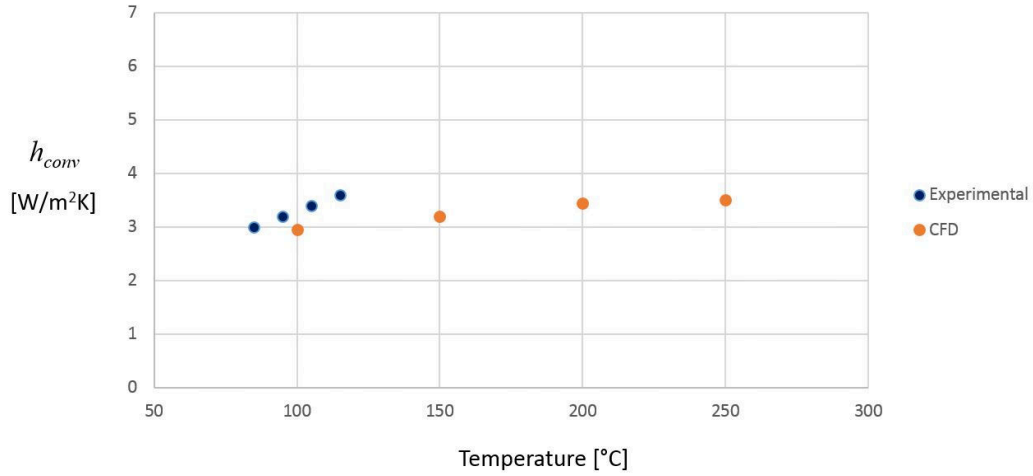

Figure 17 Solid disc: Experimental and CFD average convective heat transfer coefficients

6. Discussions

Conducted CFD analyses under-predicted the values of the convective heat transfer coefficients. This was particularly the case for the ventilated disc, which has much more complex flow patterns. It was also established that ventilated disc has higher values of the convective heat transfer coefficient, with this design also having much higher total wetted area. The combined effects will considerably increase convective dissipation but higher thermal capacity of this disc must be also considered. Ventilated disc has approximately 1.8 times higher wetted area and 2.9 times higher mass. Overall, the indications are that the two designs would cool at relatively similar rate in still air, from the same initial temperatures. This might change on the vehicle but generally is a good sign as of maintaining relatively comparable temperatures of the front and rear brakes.

In addition to the VW Passat front and rear discs, it is interesting to present measured values of the two Lotus Elise S2 disc designs. As no CFD analyses were conducted for these discs, only experimental values are presented in Table 3, for comparison reasons along VW Passat discs.

Table 3 Measured average convective heat transfer coefficients for four designs studied

Ref. Fig. 1	Disc design	h_{conv} [W/m^{2}K]			
		Temperature range [°C]			
		120 - 110	*110 - 100*	*100 - 90*	*90 - 80*
a)	Ventilated with radial vanes	5.3	5.0	4.8	4.5
b)	Solid	3.6	3.4	3.2	3.0
c)	Ventilated with curved vanes	4.2	3.8	3.7	3.5
d)	Ventilated with curved vanes; cross drilled	4.4	4.1	3.7	3.5

The overall h_{conv} values (Table 3) indicate that the disc with radial vanes (VW Passat front) has the highest cooling rates and the solid disc (VW Passat rear) the lowest. Curved vanes help in increasing air flow and convective cooling of rotating discs but in stationary conditions curved vanes trap the air, preventing the buoyant flow upwards. It is also interesting to see (Table 3) that cross drilling has practically no influence at lower temperatures up to about 100°C but at higher temperatures there is a measurable improvement of about 5% at 120°C. CFD analyses were not performed for curved vane discs but some of the following photographs effectively illustrates air flow in stationary cooling.

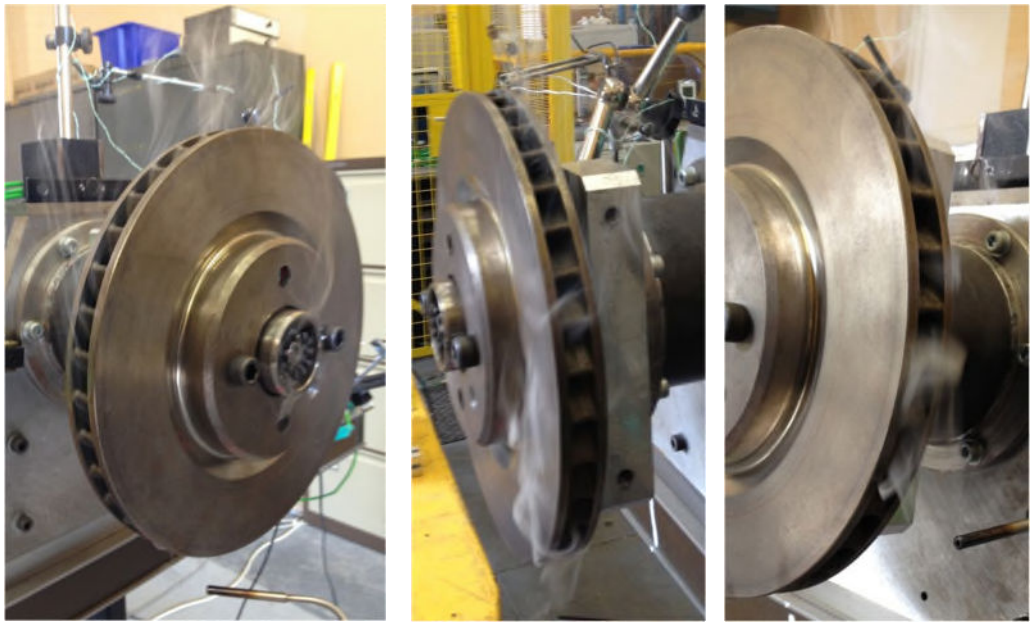

a) **b)** **c)**

Figure 18 Curved vane standard disc smoke tests:
(a) Flow channels pointing upwards; **(b)** and **(c)** Flow channels pointing downwards;

Figure 18 effectively illustrates the problem with stationary cooling of the curved vane discs. At the mid horizontal plane, at the end where the flow channels (and vanes) point upwards (18a), the upwards flow is reasonable and seems very steady. The smoke is rising smoothly. However, at diametrically opposite end (18b and c) where the vanes point downwards, there is obvious slowing down of the flow and chocking. The smoke is stagnant. The flow through the bottom and top of the ventilation channels is not particularly good either.

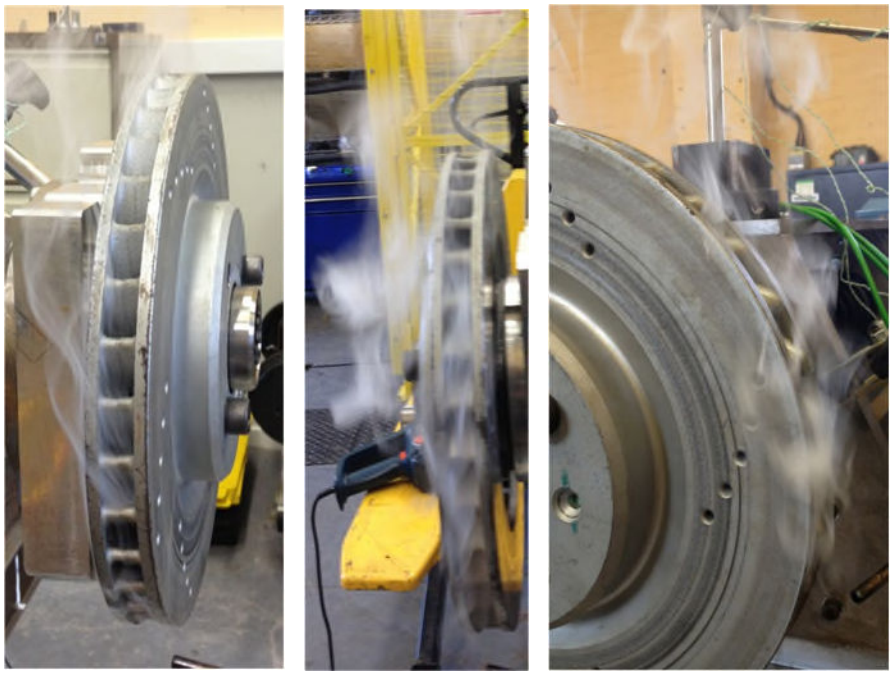

a) **b)** **c)**

Figure 19 Curved vane cross drilled disc smoke tests:
(a) Flow channels pointing upwards; **(b)** and **(c)** Flow channels pointing upwards;

Figure 19 presents cross drilled disc, showing a similar flow problems to the standard, non-drilled disc (Figure 18). At the mid horizontal plane, at the end where the flow channels (and vanes) point upwards (19a), the flow is reasonable and seems very steady, similarly to the non-drilled disc (Figure 18a). However, at the diametrically opposite end (19b and c), there is obvious obstruction and chocking. To a certain degree the holes drilled through friction faces help the flow and in Figure 19c there is a clear view of the smoke rising upwards through the cross drilled holes. It is reasonable to assume that in some areas the holes will also provide air entry, helping the overall cooling. The effects are expected to be more pronounced with increased buoyancy, and the values in Table 3 prove that, with the cross drilled disc showing superior cooling characteristics at higher temperatures (in comparison to the standard disc). The flow through the bottom and top of the ventilation channels can be also marginally helped with cross drilling.

7. Conclusions

Experimental investigation of the heat dissipation from stationary discs was successful in ensuring repeatable and accurate measurement and prediction of the total, convective and radiative heat dissipation coefficients. The values compare favourably with CFD analyses, though the differences are somewhat pronounced for the ventilated discs. The speeds of the hot air rising above the disc are far too low and flow pattern narrow and relatively irregular, making the validation of air speeds and air temperatures practically impossible. However, the use of smoke generator (with neutral buoyancy smoke) and suitable probe was very useful in qualitatively validating the flow patterns.

Convective heat transfer coefficients increase with temperature but the values are very low, typically between 3 and 5 W/m^2K for the disc designs and temperature range analysed. As expected, from the

four designs studied, the disc with radial vanes has highest convective heat dissipation coefficient and the solid disc the lowest. The reduction is about 30%, with the disc with curved vanes values being about 20% lower than for the disc with radial vanes.

Cross drilling of the disc with curved vanes seems to only marginally improve static cooling, predominantly at higher temperatures.

Low values of convective heat transfer coefficients indicate low dissipated power (heat), in particular for the solid disc. Consequently, cooling times are very long and the contribution of the other two heat dissipation modes, conduction and radiation higher. At high disc temperatures (>400°C), radiative losses in stationary conditions can be an order of the magnitude higher than convective.

When installed on the vehicle, with the addition of the caliper assembly, wheel, mudguard and dust shield, the cooling of brake discs is likely to be even further reduced. Future work is concentrated in addressing this challenge in two ways, by improving CFD modelling and equipping the Thermal Spin Rig with induction heater to heat the disc much more rapidly and to much higher temperatures.

References

Churchill, S.W. and Chu, H.H.S. (1975), Correlating Equations for Laminar and Turbulent Free Convection from a Horizontal Cylinder. *International Journal of Heat Mass Transfer,* 18(9), 1975,1049-1053.

Cobb, E. C. and Saunders, O. A. (1959), Heat transfer from a rotating disk. Proceedings of the Royal Society of London A: Mathematical, Physical and Engineering Sciences, 236(1206), pp. 343-351, 1956.

Daudi, A.R. (1992), 72 Curved Fins and Air Director Idea Increse Airflow through Brake Rotors, SAE Paper 1999-01-0140, 1999.

Dufrenoy, P., Berte, E., Witz, J-F. and Desplanques, Y. (2018), A New Camera for Quantitive Measurements of Temperature and Emissivity During Braking, Paper EB2018-VDT-033, EuroBrake Conference, 22-24 May 2018, The Hague, Netherlands,

Eisengräber, R., Grochowicz J. et al. (1978), Comparison of different methods for the determination of the friction temperature of disc brakes (No. 1999-01-0138). SAE Technical Paper, 1999.

Galindo-Lopez, C.H. and Tirovic, M. (2008) Understanding and improving the convective cooling of brake discs with radial vanes. Proc IMechE Part D: Journal of Automobile Engineering, vol. 22, no. D7, 2008, 1211-1229.

Galindo-Lopez, C. H. and Tirovic, M. (2013) 'Maximizing heat dissipation from ventilated wheel-hub-mounted railway brake discs', Proc. Instn. Mech. Engrs. Part F, Journal of Rail and Rapid Transit, Volume 227, Issue 3, pp. 269-285.

Grieve, D. G., Barton, D. C., Crolla, D. A. and Buckingham, J. T. (1998), Design of a lightweight automotive brake disc using finite element and Taguchi techniques. Proceedings of the Institution of Mechanical Engineers, Part D: Journal of Automobile Engineering, 212(4), pp. 245-254, 1998.

Limpert, R. (1975), Cooling analysis of disc brake rotors (No. 751014). SAE Technical Paper, 1975.

McAdams, W.H. (1954), Heat Transfer, McGraw-Hill, 1954.

Morgan, V.T. (1975), The Overall Convective Heat Transfer from Smooth Circular Cylinders. Advances In Heat Transfer, 1975, 199-264.

Morgan, S. and Dennis, R. W. (1972), A theoretical prediction of disc brake temperatures and a comparison with experimental data (No. 720090). SAE Technical Paper, 1972.

Necati Özisik, M. (1989), *Heat Transfer A Basic Approach.* McGraw-Hill, 1989.

Newcomb, T. P., Transient temperatures attained in disk brakes. British Journal of Applied Physics, 10(7), pp. 339-340, 1959.

Newcomb, T. P. and Spurr, R. T., Braking of road vehicles. s.l (1967).: Chapman & Hall. 1967.

Noyes, R. N. and Vickers, P. T. (1969), Prediction of surface temperatures in passenger car disc brakes (No. 690457). SAE Technical Paper, 1969.

Olphe-Galliard, M. (2011), Study of Thermodynamics and Fluid Mechanics Involved in the Cooling of Brake Discs, MSc Thesis, Cranfield University 2011, UK.

Pevec, M., Potrc. I., Bombek, G., Vranesevic, D. (2012), Prediction of the cooling factors of a vehicle brake disc and its influence on the results of a thermal numerical simulation. Int. J. Automobile Technol, 2012, (13)5: 725–733.

Richardson, P. D. and Saunders, O. A. (1963), Studies of flow and heat transfer associated with a rotating disc. Journal of Mechanical Engineering Science, 5(4), pp. 336-342, 1963.

Sisson, A. E. (1978), Thermal analysis of vented brake rotors (No. 780352). SAE Technical Paper, 1978.

Son, J.K., Jung Y-S. and Jeon, H-h., Optimization Analysis and Design of Brake Cooling System (2018), Paper EB2018-SVM-003, EuroBrake Conference, 22-24 May 2018, The Hague, Netherlands.

Stevens, K. (2013), An Investigation into Heat Dissipation from a Stationary Commercial Vehicle Brake Disc in Parked Conditions - EngD Thesis, Cranfield University, 2013.

Stevens K. and Tirovic M. (2018), Heat dissipation from a stationary brake disc, Part 1: Analytical modelling and experimental investigations, Proc IMechE Part C: J Mechanical Engineering Science, Vol. 232(9) 1707–1733, 2018.

Tang, J., Bryant, D. and Qi, H., Experimental Investigation of the Dynamic Thermal Deformation and Judder of a Ventilated Disc Brake (2018), Paper EB2018-FBR-002, EuroBrake Conference, 22-24 May 2018, The Hague, Netherlands.

Teimourimanesh S., Vernersson, T. and Lunden, R., Modelling of temperatures during railway tread braking: Influence of contact conditions and rail cooling effect (2014), Proc. Instn. Mech. Engrs. Part F, Journal of Rail and Rapid Transit, Vol. 228 (1) 93-109, 2014.

Tirovic, M. and Stevens, K. (2018) 'Heat dissipation from a stationary brake disc, Part 2: CFD modelling and experimental validations', Proc IMechE Part C: J Mechanical Engineering Science 2018, Vol. 232(10) 1898–1924.

Tirovic, M. and Voller, G.P. (2005), Interface pressure distributions and thermal contact resistance of a bolted joint, Proceedings of The Royal Society, Series A (2005) 461, pp. 2339-2354.

Topouris, S. (2017) Design and Optimisation of a High Performance Lightweight Monoblock Cast Iron Brake Disc, PhD Thesis, Cranfield University, 2017.

Wagner, C. (1948), Heat transfer from a rotating disk to ambient air. Journal of Applied Physics, 19(9), pp. 837-839, 1948.